Characterization of Three Distinct Catalytic Forms of Human Tryptase-β: Their Interrelationships and Relevance[†]

Norman M. Schechter,*[,‡,§] Eun-Jung Choi,[‡] Trevor Selwood,[‡] and Darrell R. McCaslin[||]

Department of Dermatology and Department of Biochemistry and Biophysics, University of Pennsylvania, Philadelphia, Pennsylvania 19104, and Biophysics Instrument Facility, Department of Biochemistry, University of Wisconsin, Madison, Wisconsin 53706

Received March 8, 2007

ABSTRACT: Human tryptase-β (HTβ) is a serine protease that is isolated as a tetramer of four identical, catalytically active subunits (HTβ-AT). Tetramer activity is not affected by protein-based physiological inhibitors but instead may be regulated by an autoinactivation process we have called spontaneous inactivation. Unless stabilized by heparin or high salt, the active tetramer converts to an inactive state consisting of an inactive-destabilized tetramer that reversibly dissociates to inactive monomers upon dilution. We refer to this mixture of inactive species as siHTβ and show in this study that previous reports of monomeric catalytic forms are derived from this mixture. siHTβ itself did not hydrolyze model substrates but unlike the tetramer did react slowly with the serpin α2-antiplasmin (α2-AP), suggesting a highly limited catalytic potential. In the presence of heparin (or other highly charged polysaccharides), we demonstrate that siHTβ formed a well-defined complex with the heparin (siHTβ-HC) that reacted 70-fold faster with α2-AP than siHTβ and also hydrolyzed model substrates and fibrinogen. Formation of siHTβ-HC was limited to dilute subunit solutions since high subunit concentrations resulted in the reformation of the active tetramer. By compensating for changes in the strength of heparin binding, siHTβ-HC could be formed over the pH range of 6.0−8.5. The activity dependence on pH was bell-shaped with highest activity between pH 6.8 and pH 7.5. In contrast, HTβ-AT activity showed no dependence upon heparin, increased over the pH range of 6.0−8.5, and was much higher than that of siHTβ-HC especially above pH 6.8. HTβ-AT incubated with excess heparin of different size (3−15 kDa) was functionally stable at 25 °C but lost activity regardless of heparin size at 37 °C above pH 6.8. The change in stability, which is likely due to weakened heparin binding, did not result in the formation of a stable catalytic monomer. These results confirm that siHTβ is for the most part an inactive species and that any active monomer is a consequence of heparin binding to siHTβ under dilute conditions where unfavorable thermodynamics and/or kinetics restrict formation of active tetramer. Heparin binding under these conditions drives a limited reorganization of the active site to a conformation that is catalytic but not the equivalent of a subunit within the active tetramer.

HTβ,[1] a trypsin-like serine protease expressed by mast cells (*1*, *2*), has several structural forms. The protease whether isolated from tissues or recombinant expression systems is a tetramer of four identical catalytic subunits (*3*−*10*). The active tetramer (HTβ-AT) can hydrolyze many peptide-NA substrates with high efficiency (*11*, *12*). This activity is inhibited by small competitive inhibitors such as pAb and leupeptin (*4*, *10*, *13*−15) but not by protein-based inhibitors, such as the tight-binding inhibitors SBTI and BPTI, or irreversible inhibitors, such as serpins (*4*, *10*, *13*, *16*). The crystal structure of HTβ-AT revealed an unusual ring-like tetramer in which the active sites of the subunits face a central aqueous pore (*7*). Because proteins cannot easily enter the pore, steric hindrance likely prevents access of protein-based inhibitors to the active sites.

Another structural form is the product of a process we have called spontaneous inactivation. While HTβ-AT is functionally stable in high salt solution, it rapidly loses activity in low salt unless heparin, a highly negatively charged GAG, is present (*3*, *17*, *18*). Activity loss is a first-order process dependent on NaCl concentration, temperature, and pH (*17*−20). Under conditions approximating physiological, inactivation is rapid ($t_{1/2}$ ≈1.0 min), suggesting that

[†] This work was supported by NIH Grant AI45075.

* Address correspondence to this author at the Department of Dermatology, University of Pennsylvania. Phone: 215-898-3680. E-mail: schechte@mail.med.upenn.edu. Fax: 215-573-2033.

[‡] Department of Dermatology, University of Pennsylvania.

[§] Department of Biochemistry and Biophysics, University of Pennsylvania.

[||] Department of Biochemistry, University of Wisconsin.

[1] Abbreviations: AEBSF, 4-(2-aminoethyl)benzenesulfonyl fluoride; α2-AP, α2-antiplasmin; BPTI, bovine pancreatic trypsin inhibitor; GAG, glycosaminoglycan; IPR-NA, H-D-Ile-Pro-Arg-NA; HTβ, human tryptase-β; HTβ-AT, human tryptase-β active tetramer; k_{assoc}, apparent second-order rate constant for association; K_d, equilibrium dissociation constant; k_{obs}, observed pseudo-first-order rate constant; L-BAPNA, N^{α}-benzoyl-L-Arg-NA; MW, molecular weight; NA, *p*-nitroanilide; pAb, *p*-aminobenzamidine; SBTI, soybean trypsin inhibitor; SEC, size exclusion chromatography; siHTβ, spontaneously inactivated HTβ; siHTβ-HC, complex of siHTβ with heparin; SucAAPR-NA, Suc-Ala-Ala-Pro-Arg-NA; SucAAPK-NA, Suc-Ala-Ala-Pro-Lys-NA; TosGPK-NA, N-*p*-tosyl-Gly-Pro-Lys-NA; Z-Lys-SBzl, benzyloxycarbonyl-Lys-thiobenzyl ester.

10.1021/bi7004625 CCC: $37.00
Published on Web 07/27/2007

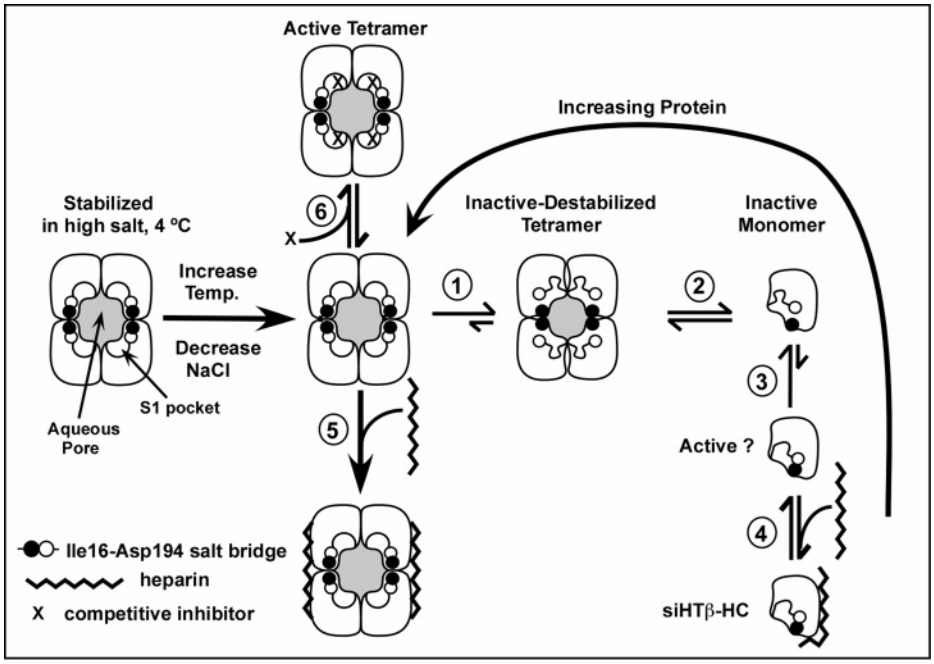

FIGURE 1: Model describing the interrelationships between HTβ-AT and the products of spontaneous inactivation. HTβ-AT is a tetramer with active sites facing a central pore. Spontaneous inactivation is initiated upon dilution of HTβ-AT stabilized by high salt at 4 °C into a solution of low salt and elevated temperature (decay conditions). Under decay conditions, structural changes occur that disrupt the S1 pocket and possibly the Ile16−Asp194 salt bridge and destabilize both the large and small interface regions of the tetramer (step 1). The result is an inactive-destabilized tetramer that will dissociate upon dilution (step 2). The inactive-destabilized tetramer and its dissociated form(s) are collectively called siHTβ. Catalytically active forms derived from siHTβ are depicted in steps 3 and 4. Step 3 is an energetically unfavorable isomerization to a conformation of limited activity which accounts for the slow reaction of siHTβ with the serpin, α2-AP. Step 4 is an interaction of very dilute siHTβ with heparin to produce a complex, siHTβ-HC, that reacts faster with α2-AP than monomeric siHTβ and is capable of hydrolyzing peptide−NA and protein substrates but is not equivalent to a subunit within the active tetramer. Stabilization of the active tetramer by heparin and competitive inhibitors is depicted as steps 5 and 6. These interactions also drive reformation of the active tetramer from siHTβ. Step 5 is presented as irreversible because over prolonged periods of incubation at 25 °C heparin−HTβ-AT complexes show little, if any, loss of activity and remain resistant to inhibition by protein-based inhibitors. At 37 °C, step 5 is reversible above pH 6.8 as spontaneous inactivation is observed in the presence of heparin. The long curved arrow indicates that in the presence of heparin or competitive inhibitors HTβ-AT will be favored at high siHTβ concentrations, thereby limiting the formation of significant quantities of siHTβ-HC to relatively low siHTβ concentrations.

spontaneous inactivation could function as a self-regulatory mechanism (*17*, *19*). Our physical studies indicate that inactivation occurs within the tetramer, as a result of conformational changes that disrupt critical active site features including the major substrate binding site (S1 pocket) (*5*, *9*, *10*, *15*) and possibly the Ile16−Asp194 salt bridge (*5*, *15*). The events associated with spontaneous inactivation also reduce the stability of the tetramer (*5*, *10*). Thus, in the model of Figure 1 an inactive tetramer is shown as the first species formed in spontaneous inactivation (step 1). This destabilized tetramer, unlike HTβ-AT, is in equilibrium with inactive monomers (step 2), which become the predominant species when the total subunit concentration is below 1.0 μM (*5*, *10*). We refer to the mixture of inactive HTβ species resulting from spontaneous inactivation as siHTβ.

The conformational changes associated with spontaneous inactivation are reversible since ligands that stabilize HTβ-AT, such as heparin (step 5), can mediate reformation of active tetramer from siHTβ (*5*, *15*, *17*, *18*, *20*). Additionally, we have demonstrated that small competitive inhibitors that bind primarily to the S1 pocket stabilize the active tetramer structure (step 6) as well as mediate its reformation from siHTβ (*10*). These small competitive inhibitors cannot bind to multiple subunits as has been proposed for heparin. Therefore, their stabilization of the active tetramer instead of monomeric species provides strong evidence that the tetramer is the preferred active form of HTβ.

A number of recent studies have reported a monomeric form(s) of HTβ with enzymatic activity that unlike HTβ-AT is sensitive to protein-based inhibitors (*18*, *21*−25). Such a species appears inconsistent with our studies in which monomers are generated only by dissociation of the inactive-destabilized tetramer (Figure 1). These studies have not been consistent in identifying the origin of the catalytic monomer, reporting its generation only at low pH by addition of heparin to inactivated HTβ (*24*, *25*) as well as by direct dissociation at pH 7.5 of the heparin-stabilized tetramer (*21*, *23*). Unusual for a serine protease and unlike HTβ-AT activity, the monomer appeared to be active only at pH 6.0 and highly specific for the model peptide substrate IPR-NA. Thus, further work was needed to fully understand the origin of a HTβ catalytic monomer, its catalytic properties compared to the active tetramer, and its physiological relevance.

We have shown that the ability of heparin and small molecule inhibitors to mediate reformation of the active tetramer decreases as the siHTβ concentration in the incubation decreases (*10*, *15*, *17*). At highly dilute siHTβ concentrations ($\approx$0.1 μM) where monomer is virtually the only siHTβ species, significant reformation of the active tetramer does not occur unless both heparin and small molecule inhibitors are added to the incubation (*10*). Thus, at low siHTβ concentration there is a potential for heparin to interact with the monomer without reformation of the active tetramer.

In the current study, the catalytic potential of siHTβ is investigated. We confirm that siHTβ itself does not hydrolyze model peptide substrates but can react with serpins possibly as the result of an induced-fit mechanism. Moreover, at dilute siHTβ concentrations where the tetramer does not reform, the monomer interacts with heparin (and other highly charged polysaccharides) to produce a well-defined complex (siHTβ-HC) that reacts faster with serpins than siHTβ and hydrolyzes the same model substrates as HTβ-AT, although with much less efficiency especially at pH $\geq$7.0. We suggest that heparin binding to dilute siHTβ along with other factors (pH, NaCl concentration, temperature) functions to drive the conformation of siHTβ toward that of an active subunit, producing a suboptimal "crippled" catalytic species relative to a subunit within the active tetramer. Only conformational changes associated with tetramer formation can restore full catalytic function.

EXPERIMENTAL PROCEDURES

Materials. Substrates were purchased from Bachem, Philadelphia, PA, or Sigma, St. Louis, MO. Aprotinin (BPTI) and dextran sulfate (average mass 8 kDa) were purchased from Sigma. Heparin (average mass 3, 5, and 15 kDa), dermatan sulfate (30 kDa, porcine mucosa), chondroitin sulfate A (50 kDa, bovine trachea), and bovine fibrinogen were purchased from Calbiochem, La Jolla, CA. The serpin α2-AP was from Athens Biochemicals, Athens, GA. Gelcode blue was obtained from Pierce, Rockford, IL.

HTβ and siHTβ. All studies were preformed with recombinant HTβ expressed and characterized as described previously (*9*, *26*). HTβ-AT and siHTβ concentrations reported in the text refer to subunits (MW = 27500), rather than tetramers. The concentration of active HTβ-AT subunits was measured using previously determined specific activities for subunit hydrolysis of L-BAPNA or TosGPK-NA (*9*). Purified recombinant HTβ-AT was greater than 90% active as determined by comparison of its concentration measured by activity with that measured by A_{280} [ϵ_{280nm}(HTβ subunit) = 64900 M^{-1} cm^{-1}] (*9*). To produce siHTβ, stock protease stabilized in 2 M NaCl (40−80 μM in 2 M NaCl, 0.01 M MOPS, pH 6.8) was diluted to 1.0−8.0 μM in 0.2 M NaCl and 0.01 M MOPS, pH 6.8, and incubated at 37 °C for 30 min followed by cooling to 25 °C. Since siHTβ formed as above could be quantitatively converted back to HTβ-AT, the total concentration of siHTβ was assumed equivalent to HTβ-AT prior to decay. siHTβ levels remained constant in decay solution for 1−2 days at 25 °C based on the ability to generate siHTβ-HC in the IPR-NA assay as discussed below.

Enzymatic Assays. Hydrolysis of model substrates in a 1 cm pathlength cuvette was monitored in a Beckman DU 640 spectrophotometer at 25 °C. Assays typically were in a total volume of 250 μL containing 0.1 or 0.2 M NaCl and 0.1 M buffer (MES, pH 6.0, MOPS, pH 6.8, HEPES, pH 7.5, Tris or Tricine, pH 8.0, Tris or CHES, pH 8.5), 0.005% dodecyl maltoside, 9.0% Me_2SO, and GAG or dextran sulfate as indicated in the text. NaOH was used to titrate acid forms of buffers to the desired pH, and HCl was used to titrate Tris base. Buffers were chosen to produce pHs near their pK_a's to keep their contribution to the ionic strength of solutions relatively constant. Hydrolysis of peptide-NA and L-BAPNA was monitored at 410 nm where ϵ_{410nm}(NA) = 8800 M^{-1} cm^{-1}. Activity measurements were usually initiated by addition of 1−5 μL of HTβ-AT stabilized in high salt or siHTβ in decay buffer to the assay medium to produce a final subunit concentration of 10 nM. Initial rates were measured over a 2−7 min period during which <20% of the substrate was consumed. Assays of siHTβ with heparin present showed an initial upward curvature in product accumulation that became linear after 2−3 min. Initial velocity measurements were based on this "steady"-state rate. The curvature was eliminated by preincubation of siHTβ in assay medium containing heparin, suggesting that it may reflect the rate of conversion of siHTβ to siHTβ-HC. Sensitivity to BPTI was typically measured by addition of the inhibitor to the assay after steady state was achieved. Percent reduction in activity is reported.

Reformation of the Tetramer from siHTβ by Heparin. Reformation of active tetramer was assessed by incubation of 0.1−4.0 μM siHTβ in 1.0 mg/mL heparin, 0.1 M NaCl, and 0.05 M buffer, pH 6.0−8.0. The pH in the incubation was adjusted to the final value by the addition of 1.0 M stock buffer (MES, pH 6.0, MOPS, pH 6.8, MOPS, pH 7.5, or Tris, pH 8.0). For activity measurement, aliquots from incubations were diluted into assay buffer to a final subunit concentration of 10 nM, and initial velocities using various substrates were measured in the absence and presence of BPTI. These values were compared to the activity of 10 nM siHTβ in the absence and presence of BPTI to estimate the extent of tetramer reformation. Reformation was considered complete after an overnight incubation; incubations monitored periodically usually reached a maximum level of activity between 0.5 and 3 h and remained constant for >24 h.

Determination of Kinetic and Binding Constants. Kinetic constants were determined from plots of initial velocity vs substrate concentration ($[S]_0$) by fitting data to the Michaelis−Menten rate equation. Data sets consisted of 10 measurements mostly at different $[S]_0$ ranging from 0.1 to 2.0 mM. The hyperbolic increase in siHTβ activity with increasing concentrations of polysaccharide was analyzed using the simple binding expression (eq 1). Fits of the data were used to determine V_{lim}, a maximal hydrolytic rate, V_0, the rate of hydrolysis in the absence of polysaccharide, and K_d, an apparent equilibrium dissociation constant for the binding of polysaccharide to siHTβ. Total polysaccharide concentrations in binding reactions were always in excess of the siHTβ subunit concentration by at least 10-fold, except for the two lowest concentrations of dextran sulfate. The average MW from the supplier was used to calculate polysaccharide concentrations. The apparent rate constant for the inhibition of siHTβ-HC by α2-AP was determined at 25 °C using the progress curve method (*27*). Reactions were initiated by the addition of siHTβ (10 nM) to a cuvette containing substrate (1 mM IPR-NA), heparin (1.0 mg/mL), buffer (0.1 M Tris, pH 8.0, 0.1 M NaCl, 0.005% dodecyl maltoside, 9% Me_2SO), and excess inhibitor ($[I]_0 \gg 10[\text{siHT}\beta]_0$). Absorbance at 410 nm (A) resulting from substrate turnover was monitored with time (t), and the data were fit to eq 2 to determine the parameters k_{obs}, the observed pseudo-first-order rate constant for loss of activity, A_0, the initial absorbance, v_0, the activity at time 0, and v_s, the activity at steady state; k_{assoc}, the apparent second-order rate constant for association, was then calculated using eq 3. The K_m was determined in

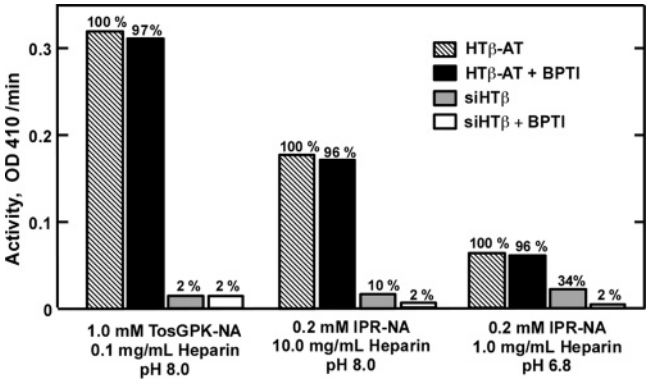

FIGURE 2: Hydrolytic activity and BPTI sensitivity of HTβ-AT and siHTβ. HTβ-AT stabilized in high salt or 1.0 μM siHTβ produced as described in Experimental Procedures was added to assays to give a final subunit concentration of 10 nM. Assays contained 0.2 M NaCl, 9% Me_2SO, 0.005% dodecyl maltoside, and $\pm$4.0 μM BPTI in addition to substrates, heparin (5 kDa), and pH as indicated.

a separate study. v_0 activity from fits agreed with the activity measured in the absence of inhibitor (control), and v_s was near zero, consistent with formation of an irreversible complex between protease and serpin.

$$\text{activity} = \frac{V_{\text{lim}}}{K_d/[\text{polysaccharide}]_0 + 1} + V_0 \qquad (1)$$

$$A = A_0 + v_s t + \frac{(v_0 - v_s)(1 - e^{-k_{obs}t})}{k_{obs}} \qquad (2)$$

$$k_{assoc} = \frac{k_{obs}(1 + [S]_0/K_M)}{[I]_0} \qquad (3)$$

SDS−PAGE. The reactions of various HTβ species with α2-AP and fibrinogen were analyzed by SDS−PAGE. Reactions were stopped by addition of gel sample buffer containing 1% SDS and 1.0 mM DTT followed immediately by heating at 90 °C for 5 min (*28*). Protein bands were resolved on 12% acrylamide gels (*28*) and visualized by staining with Gelcode blue.

Data Analysis. Data were analyzed by nonlinear least-squares regression using Igor Pro by Wavemetrics, Lake Oswego, OR.

RESULTS

Formation of the Catalytic Monomer. Previous studies have reported a monomeric form of HTβ that hydrolyzes the substrate IPR-NA at pH 6.0 in the presence of either 25 (*24*) or 50 μg/mL heparin (*21*, *29*). Monomer activity was distinguished from that of the tetramer by its sensitivity to protein-based inhibitors such as SBTI or BPTI. In Figure 2, we compare the hydrolytic activities of HTβ-AT and siHTβ in the absence and presence of BPTI using three sets of assay conditions. The assay with TosGPK-NA is commonly used to measure HTβ-AT activity and to monitor activity loss during spontaneous inactivation. The other two assays use IPR-NA at low and high pH but include much higher concentrations of heparin (5 kDa) than in the above studies. In all assays, the concentration of HTβ-AT or siHTβ was equivalent to 10 nM subunits, a concentration where in our studies siHTβ is fully dissociated and the active tetramer cannot be reformed by addition of heparin (*5*, *10*). This concentration was obtained by a 100-fold dilution of 1.0 μM HTβ-AT stabilized in 2 M NaCl or 1.0 μM siHTβ produced as described in Experimental Procedures into assay buffer.

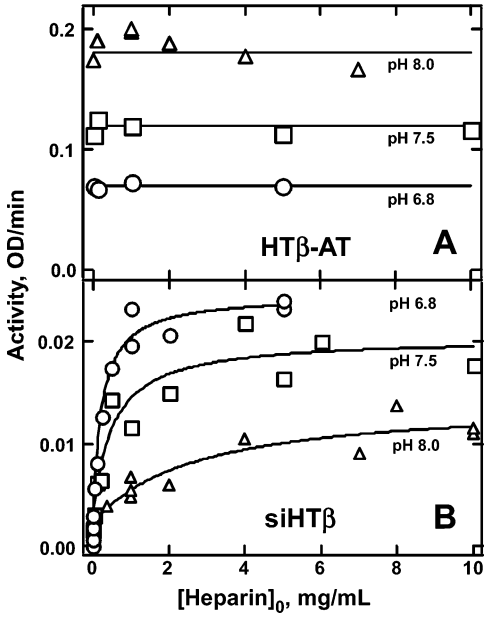

FIGURE 3: Effects of heparin concentration and pH on the hydrolysis of IPR-NA by HTβ-AT and siHTβ. Activity was measured at 25 °C with 0.2 mM IPR-NA, 0.2 M NaCl, 0.1 M buffer, 9% Me_2SO, 0.005% dodecyl maltoside, and heparin as indicated. (A) 10 nM HTβ-AT subunits (2.5 nM tetramer). (B) 10 nM siHTβ subunits. Lines in panel B are fits of eq 1 to the data.

The hydrolytic activity of HTβ-AT was only minimally affected by addition of BPTI, regardless of substrate or conditions of the assay (Figure 2). Thus, spontaneous dissociation of the tetramer did not occur upon the 100-fold dilution into assay medium. After spontaneous inactivation, 98% ($\pm$1%, $n = 8$) of the starting activity was lost when measured using the TosGPK-NA assay. The residual activity (2%) was not sensitive to BPTI and did not decay further with time. When measured using IPR-NA, activity loss from spontaneous inactivation was less than that measured using TosGPK-NA and depended on pH with a 90% ($\pm$0.5%, $n = 2$) loss at pH 8.0 but only a 66% ($\pm$7%, $n = 8$) loss at pH 6.8. Upon addition of BPTI, residual activities in both IPR-NA assays decreased to 2% ($\pm$0.5%, $n = 16$) of the rates before spontaneous inactivation, an amount similar to that observed using TosGPK-NA to assay siHTβ.

These studies demonstrate that assays using IPR-NA detect a hydrolytic activity for siHTβ that is not detected when TosGPK-NA is used as the substrate. The inhibition of this activity by BPTI is consistent with a catalytic monomer. The source of the residual 2% BPTI resistant activity in siHTβ preparations observed with all substrates is unclear.

The hydrolysis of IPR-NA by HTβ-AT and siHTβ was further characterized by a systematic examination of the effects of pH, heparin concentration, and NaCl concentration. As shown in Figure 3A, HTβ-AT hydrolysis of IPR-NA was not affected by heparin, and rates increased with pH. In marked contrast, siHTβ hydrolysis of IPR-NA was barely detectable in the absence of heparin but increased markedly to a maximal activity with increasing heparin concentration

Table 1: Effects of pH and NaCl Concentration on the Interaction of siHTβ with Polysaccharides and on IPR-NA Hydrolysis

[NaCl] (M)	pH	K_d[a] (μg/mL)	V_{lim}[b] (OD 410/ min $\times 10^3$)	V_0 (OD 410/ min $\times 10^3$)
5 kDa heparin				
0.2	6.8	200 ± 40	24 ± 1	0.9 ± 0.6
0.1	6.8	2.0 ± 0.5	50 ± 4	7 ± 3
0.2	7.5	500 ± 250	19 ± 1	1.5 ± 0.2
0.1	7.5	4.0 ± 0.6	70 ± 3	5 ± 2
0.2	8.0	4000 ± 1200	12 ± 2	2 ± 0.5
0.1	8.0	160 ± 40	35 ± 3	4 ± 2
0.1	8.5	900 ± 30	11 ± 0.6	2.1 ± 0.4
3 kDa heparin				
0.1	6.8	3.0 ± 0.3	58 ± 2	8 ± 2
0.1	8.0	250 ± 60	39 ± 3	5 ± 1
30 kDa dermatan sulfate				
0.1	6.8	12 ± 5	45 ± 5	5 ± 3
0.1	8.0	1100 ± 30	27 ± 3	5 ± 1
8 kDa dextran sulfate				
0.1	6.8	0.10 ± 0.04	60 ± 7	9 ± 1

[a] Parameters and errors are from fits to eq 1 of data in Figures 3 and 4 and other data not shown. [b] All assays contained 10 nM subunits.

(Figure 3B). This hyperbolic dependence of activity on heparin concentration was well described by eq 1 (solid lines in Figures 3B and 4A), thereby implying a direct link between siHTβ hydrolytic activity and saturation of a well-defined, heparin binding site on monomeric siHTβ. Apparent binding constants (K_d) and maximal hydrolytic rates (V_{lim}) obtained from fits of the data to eq 1 are reported in Table 1. Also in contrast to HTβ-AT, maximal hydrolytic rates for siHTβ decreased with increasing pH and were substantially less than those of HTβ-AT at the same pH (e.g., compare *y*-axis values in panels A and B of Figure 3 and see Figure 5). K_d values also increased with increasing pH; thus, not only are maximal activities of the catalytic monomer (siHTβ-HC) low at high pH but higher heparin concentrations are required to attain these activities.

Decreasing the NaCl concentration in assays from 0.2 to 0.1 M decreased the concentration of heparin required for maximal activity (lowered K_d) and increased the limiting activity about 2.0−3.0-fold depending on pH (Figure 4A and K_d and V_{lim} values in Table 1). The maximal activities of siHTβ-HC in 0.1 M NaCl were >95% sensitive to BPTI (data not shown), showing that the higher catalytic rates were not due to reformation of the active tetramer. HTβ-AT activity increased only slightly when assayed in lower salt (compare activities in Figure 3A with those in Figure 5) but remained substantially higher than siHTβ-HC activity over the pH range (also see Table S1, Supporting Information). Thus, siHTβ-HC activity is more highly affected by NaCl concentration than HTβ-AT activity.

In addition to 5 kDa heparin, a variety of polysaccharides, including 3 kDa heparin, dextran sulfate (8 kDa), and dermatan sulfate (30 kDa), were able to activate siHTβ, each showing a hyperbolic dependence of activity with increasing polysaccharide concentration (Figure 4B). On the basis of K_d values, dextran sulfate, the most highly sulfated polysaccharide, was the most efficient activator followed by 3 and 5 kDa heparin, which had similar K_d values, and dermatan sulfate with the lowest K_d value. Chondroitin sulfate (50 kDa), the least sulfated polysaccharide, did not produce

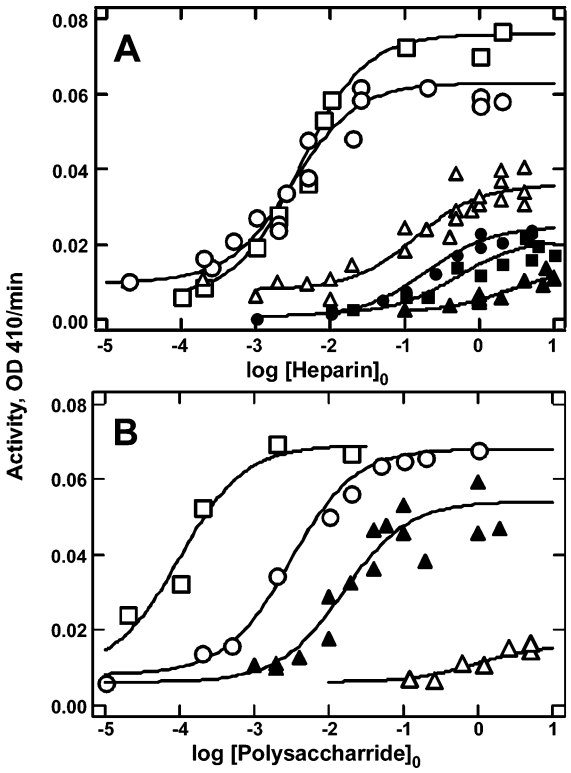

FIGURE 4: Effect of polysaccharide concentration, NaCl concentration, pH, and type of polysaccharide on the activity of siHTβ. Assays contained 0.2 mM IPR-NA, 0.1 M buffer, 9% Me_2SO, 0.005% dodecyl maltoside, NaCl, and polysaccharide (mg/mL) as indicated and were initiated by dilution of 1.0 μM siHTβ into assay medium to a final concentration of 10 nM subunits. (A) Circles, boxes, and triangles are rates at pH 6.8, 7.5, and 8.0, respectively, using 5 kDa heparin; filled symbols are rates in 0.2 M NaCl, and open symbols are in 0.1 M NaCl. (B) Polysaccharides were dextran sulfate (boxes), 3 kDa heparin (circles), dermatan sulfate (solid triangles), and chondroitin sulfate (open triangles), and the pH was 6.8.

significant activation. Maximal activities with different activating polysaccharides were similar (0.053 ± 0.007 OD/min) despite K_d values that varied 20−120-fold (Table 1, 0.1 M NaCl, pH 6.8 data). Activities generated with all polysaccharides were sensitive to BPTI (data not shown). Thus, activation of monomeric siHTβ is a property of highly charged polysaccharides with the binding of each producing a species of comparable catalytic ability.

Characterization of siHTβ-HC Catalytic Activity. The kinetic parameters for hydrolysis of IPR-NA by HTβ-AT and siHTβ-HC were determined at pH 6.8 and 8.0. Heparin concentrations in these studies and in most of those to follow were sufficient (1.0 mg/mL) to provide maximal (or nearly maximal) rates for siHTβ. Plots of initial velocities vs $[S]_0$ were hyperbolic, and the derived kinetic parameters are reported in Table 2. The most notable difference between the two catalytic forms was in k_{cat}. k_{cat} values for HTβ-AT were higher than those for siHTβ-HC and increased approximately 2-fold between pH 6.8 and pH 8.0, while those for siHTβ-HC did not increase with pH. K_m values for the two species were essentially identical at pH 6.8 but differed at pH 8.0 as the K_m for HTβ-AT decreased slightly while that for siHTβ-HC increased approximately 1.5-fold. Thus, relative to HTβ-AT activity, high pH negatively affected siHTβ-HC activity by limiting k_{cat} and raising K_m.

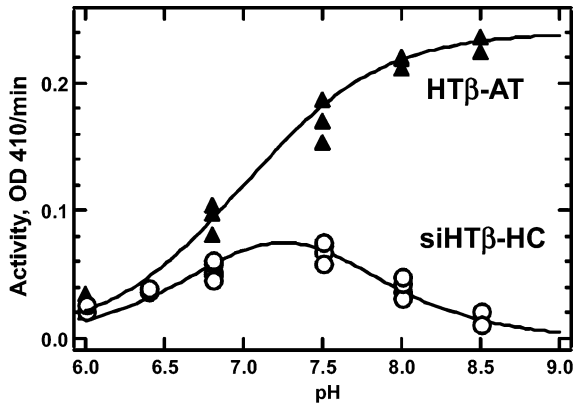

FIGURE 5: Effect of pH on the activity of HTβ-AT and siHTβ-HC. 10 nM subunits of each species were assayed with 0.2 mM IPR-NA, 0.1 M buffer, 0.005% dodecyl maltoside, and 9% Me_2-SO. At each pH HTβ-AT activities were measured in the absence of heparin or in the presence of 1.0 and 5.0 mg/mL heparin. All of these measurements were within experimental error and are shown but not distinguished. The activity of siHTβ-HC was measured using similar conditions but with the heparin concentrations constant at 1.0 mg/mL, except at pH 8.5 where the concentration was increased to 4.0 mg/mL. Data were visually fit using standard equations to describe pH-related effects (*32*). The line through the HTβ-AT data assumed a pK_a of 7.0 with a limiting rate of 0.24 OD 410/min. The line for the siHTβ-HC data assumed pK_a values of 7.0 and 7.5 with a limiting rate of 0.16.

Table 2: Kinetic Parameters for the Hydrolysis of IPR-NA by HTβ-AT and siHTβ-HC

tryptase	pH	K_m (mM)	k_{cat} (s^{-1})	k_{cat}/K_m (M^{-1} s^{-1})
HTβ-AT[a]	6.8	0.81 ± 0.07[b]	97 ± 4	1.20×10^5
siHTβ-HC	6.8	0.76 ± 0.04	49 ± 1	0.65×10^5
HTβ-AT	8.0	0.62 ± 0.05	170 ± 7	2.7×10^5
siHTβ-HC	8.0	1.10 ± 0.12	50 ± 4	0.45×10^5

[a] Assays contained 10 nM subunits, 0.1 M NaCl, 0.1 M buffer, 1.0 mg/mL heparin, and 9% Me_2SO, 25 °C. [b] Errors are from fits of the data to the Michaelis−Menten rate equation.

Profiles showing the effect of pH on the hydrolysis of IPR-NA by HTβ-AT and siHTβ-HC in 0.1 M NaCl are shown in Figure 5. Substrate concentrations were below the K_m ($\approx$0.2−0.3 K_m as indicated by values in Table 2) so that activities are reflective of apparent second-order rate constants (k_{cat}/K_m). For HTβ-AT, hydrolytic rates increased with increasing pH to an apparent maximum; the curve drawn through the data assumes a pK_a of 7.0, which is consistent with the titration of His57, a key residue of the catalytic triad that governs serine protease activity (*30*−*32*). In contrast, the pH activity profile for siHTβ-HC was bell-shaped with a maximum between pH 6.8 and pH 7.5. Rates for siHTβ-HC, which are limiting activities, approached that for HTβ-AT at pH 6.0, but not at higher pH. At all pHs, including pH 6.0, HTβ-AT activity was unaffected by BPTI, while siHTβ-HC activity was more than 95% inhibited (data not shown). The difference in pH activity profiles indicates a fundamental difference in the active site structures of HTβ-AT and siHTβ-HC.

In assays containing 1 mM substrate and 1 mg/mL heparin, siHTβ-HC was shown to hydrolyze the same peptide-NA substrates as HTβ-AT, but at much lower rates (Table S1, Supporting Information). For both species, relative hydrolytic rates measured at pH 6.8 or 8.0 for five model peptide-NA

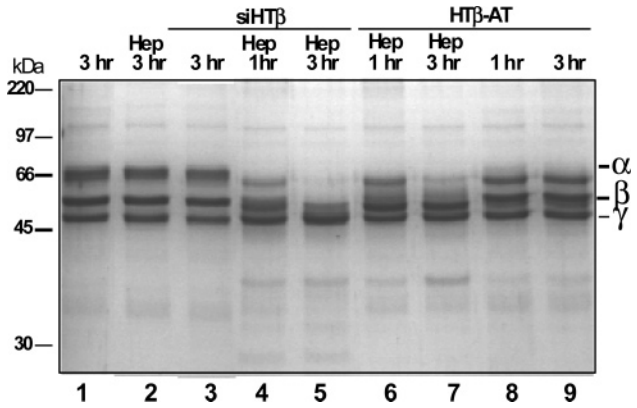

FIGURE 6: Hydrolysis of fibrinogen by siHTβ and HTβ-AT. Incubations were in a total volume of 60 μL at 25 °C, pH 6.8, with 1.0 μM fibrinogen (350 μg/mL), 0.1 M NaCl, and $\pm$1.0 mg/mL heparin (Hep). siHTβ and HTβ-AT were equivalent to 30 nM subunits; lanes 1 and 2 are controls of fibrinogen alone. Reactions were terminated by incubation for 10 min with 4.0 mM AEBSF followed by denaturation with SDS−DTT. Aliquots of 5 μL were analyzed by SDS−PAGE.

substrates followed the same order with IPR > TosGPK $\gg$ SucAAPR $\approx$ L-BAPNA $\approx$ SucAAPK. For all substrates, activities varied with pH and NaCl concentration in a manner similar to that described for the hydrolysis of IPR-NA. For HTβ-AT, rates were higher at pH 8.0 than at pH 6.8 and decreased slightly upon raising NaCl from 0.1 to 0.2 M, whereas for siHTβ-HC, rates were lower at pH 8.0 than at pH 6.8 and decreased markedly upon raising NaCl from 0.1 to 0.2 M (Table S1, Supporting Information). The hydrolytic activities of HTβ-AT and siHTβ-HC were most different at 0.2 M NaCl, pH 8.0, where siHTβ-HC hydrolyzed all substrates at rates <4% of those measured with HTβ-AT. The poor activity of siHTβ-HC under these conditions is consistent with a low maximal activity and a K_d for heparin binding higher than 1.0 mg/mL as shown in Figures 3 and 4. These results demonstrate that siHTβ-HC and HTβ-AT have similar substrate specificities and that the lower hydrolytic rates and relative effects of pH and NaCl concentration on the hydrolytic activity of siHTβ-HC are not dependent on choice of substrate.

Both HTβ-AT (*21*, *25*) and the catalytic monomer (*33*−*35*) have been shown to degrade the α and β chains of fibrinogen. In Figure 6, we show that at pH 6.8 siHTβ-HC (lanes 4 and 5), but not siHTβ (lane 3), cleaves the α and β chains of fibrinogen. The cleavage pattern was similar to that observed for HTβ-AT stabilized by heparin (lanes 6 and 7) except for the more extensive hydrolysis of the β chain, which probably reflects the greater access of protein to the active site of the catalytic monomer. Addition of BPTI to incubations blocked hydrolysis of fibrinogen by siHTβ-HC but not by HTβ-AT (Figure S1, Supporting Information). In the absence of heparin, HTβ-AT was capable of hydrolyzing only the α chain (lanes 8 and 9), a limitation noted previously (*33*). This selectivity is likely the result of spontaneous inactivation being too slow to compete with α chain cleavage but too fast to permit β chain cleavage. These studies show that siHTβ-HC as identified in our study is capable of hydrolyzing proteins.

Heparin-Mediated Reformation of HTβ-AT. The addition of heparin to siHTβ has been shown to drive reformation of the active tetramer (*10*, *17*, *18*, *20*). Thus, the formation of

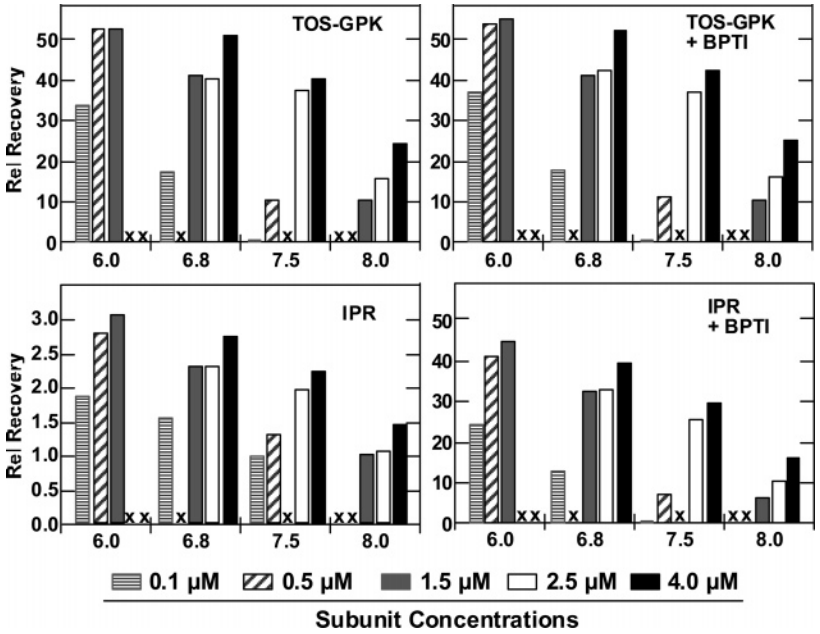

FIGURE 7: Formation of active tetramer upon incubation of siHTβ with heparin. Typically, siHTβ was incubated overnight at 25 °C in 1.0 mg/mL 5 kDa heparin and 0.1 M NaCl with pH and subunit concentrations as indicated. Subunit concentrations for which data were not collected are denoted by "x" on the abscissa. Activity measurements were initiated by dilution of aliquots from an incubation into assay medium to a final subunit concentration of 10 nM. Measurements were made in the presence and absence of BPTI using either 0.2 mM IPR-NA, 0.2 M NaCl, pH 6.8, and 1.0 mg/mL heparin or 1.0 mM TosGPK-NA, 0.2 M NaCl, pH 8.0, and 0.1 mg/mL heparin. Relative recovery is the activity for 10 nM subunits after incubation with heparin divided by a base activity determined for 10 nM siHTβ subunits before the shift to incubation conditions. For TosGPK-NA, the base activity for siHTβ in the presence and absence of BPTI was 2% of the activity before spontaneous inactivation. For IPR-NA, the base was 34% of the activity before spontaneous inactivation in the absence of BPTI and approximately 2% in the presence of BPTI.

siHTβ-HC may be limited by or compete with reformation of the active tetramer. To establish the conditions favoring reformation of the active tetramer over formation of siHTβ-HC, the effect of pH and siHTβ concentration on the recovery of the active tetramer was examined (Figure 7). Tetramer reformation was assessed in incubations containing 1.0 mg/mL heparin (5 kDa) in 0.1 M NaCl and 0.1 M buffer, pH 6.0−8.0. The heparin concentration is near that needed to saturate siHTβ (produce V_{lim}) over the range of pH being evaluated (Figure 4 and Table 1). Aliquots from incubations were assayed using both TosGPK-NA (pH 8.0) and IPR-NA (pH 6.8) ± BPTI as in Figure 2. The final subunit concentration in the assays was always 10 nM; in the presence of heparin at this subunit concentration HTβ-AT is stable and siHTβ/siHTβ-HC does not reform HTβ-AT (Figure 2).

The data reported in Figure 7 are increases relative to the activity of siHTβ measured after spontaneous inactivation and immediately prior to the shift to incubation conditions. In the assay using TosGPK-NA, which measures only HTβ-AT activity under the conditions of Figure 2, this base activity is about 2% of the activity measured before spontaneous inactivation (i.e., ~98% loss of activity) and is not sensitive to BPTI. Thus, a 50-fold increase in hydrolytic activity that is resistant to inhibition by BPTI would be equivalent to a complete return of the active tetramer. In the assay using IPR-NA, which measures HTβ-AT and siHTβ-HC activity, the activity measured after spontaneous inactivation is about 34% of the activity before spontaneous inactivation but is reduced to near 2% in the presence of BPTI. Thus, a 3-fold increase in hydrolytic activity with a 50-fold increase in activity resistant to BPTI would indicate the full return of HTβ-AT.

As shown in Figure 7, increased BPTI-resistant hydrolytic activity was observed at all pHs. The relative increases in activity and their resistance to BPTI indicate complete or near complete return of active tetramer in many instances. Both substrates gave parallel results, demonstrating that assessment of active tetramer reformation is not influenced by substrate or assay conditions used for measurement of activity. At all pHs, the extent of active tetramer reformation increased with increasing siHTβ concentration. However, at lower pH, complete recovery of the active tetramer was achieved at a lower concentration of siHTβ than at higher pH. For example, at pH 6.0, virtually full recovery of the active tetramer was observed with 0.5 μM siHTβ, whereas at pH 8.0, only 50% recovery (25-fold increase) of the active tetramer occurred in incubations with 4.0 μM siHTβ. Thus, heparin-driven reformation of the active tetramer limits the maximum concentration of siHTβ-HC that can be formed with higher pH permitting higher siHTβ-HC concentrations.

Stability of Heparin−HTβ-AT Complexes. The reformation studies just discussed indicate that heparin binding is stronger to HTβ-AT than to siHTβ-HC. In our experience, incubation of HTβ-AT with heparin (0.1−1.0 mg/mL, 5 or 15 kDa heparin, 0.2 M NaCl, pH 6.8, 25 °C) results in little loss of activity over long periods; thus, we have assumed that the interaction of HTβ-AT with heparin is virtually irreversible (Figure 1) and that heparin-stabilized HTβ-AT does not dissociate. Other studies using lower concentrations of heparin, different pH, or higher temperature have indicated that the stabilizing ability of heparin may vary depending on experimental conditions (*19*, *23*, *24*). To more completely establish the conditions under which siHTβ-HC can be generated, the functional stability of HTβ-AT in the presence of heparin was investigated at 25 and 37 °C as a function of

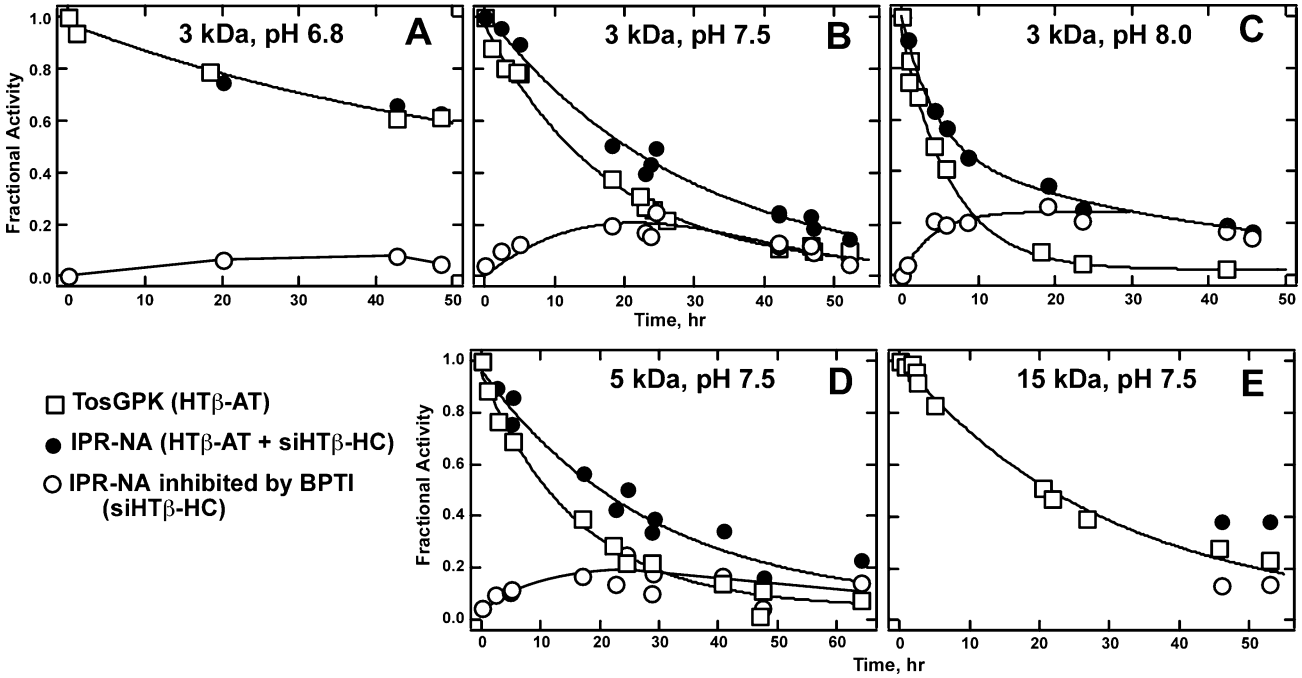

FIGURE 8: Effect of heparin size and pH on the functional stability of HTβ-AT at 37 °C. Incubations at the start contained 1.2 μM HTβ-AT, 0.2 mM heparin (based on average mass), 0.1 M NaCl, and 0.1 M buffer. Activity was measured using the TosGPK, pH 8.0, or IPR-NA, pH 6.8, assays and ±BPTI as described in Figure 2. For assay, aliquots were removed from incubations and diluted in assay medium to 10 nM HTβ subunits. Activities measured using the TosGPK-NA (squares) and IPR-NA (filled circles) assays were normalized to the activity for each substrate at time 0. The amount of IPR-NA activity inhibited by BPTI (open circles), which is zero at time 0, was normalized to the IPR-NA activity at time 0.

pH, heparin size (3, 5, or 15 kDa = 11, 17, 50 sugar moieties), and heparin concentration.

Incubations contained 1.0 μM HTβ-AT, 0.1 or 0.2 M NaCl, and either 0.02 or 0.2 mM 3 kDa (0.06 or 0.6 mg/mL), 5 kDa (0.1 or 1.0 mg/mL), or 15 kDa (0.3 or 3.0 mg/mL) heparin. Activity was monitored using both the TosGPK-NA and the IPR-NA assays ± BPTI as in Figure 2. During a 24 h incubation at 25 °C, TosGPK-NA activity, which measures only HTβ-AT, changed little (<5%) at pH 6.8 regardless of heparin size and concentration. At higher pH, a slow loss of activity (15−30% for 24 h) was observed at pH 7.5 and 8.0 in 0.02 mM heparin and 0.1 M NaCl (data not shown). This somewhat greater loss of activity above pH 6.8 suggests somewhat weaker binding of heparin to HTβ-AT at higher pH and could explain why the concentrations of siHTβ needed to reform the active tetramer at pH 7.5 and 8.0 were higher than at pH 6.8 in the reformation studies of the previous section (Figure 7). Nevertheless, the stability of HTβ-AT activity at 25 °C in the presence of heparin suggests that the interaction of HTβ-AT with heparin is tight and that complexes do not readily dissociate, at least over the pH range analyzed.

Table 3: Effect of NaCl and pH on the Inactivation Rate of Heparin-Stabilized HTβ-AT at 37 °C

heparin size (kDa)	[heparin] (mM)	[NaCl] (M)	$t_{1/2}$ (h) pH 6.8	pH 7.5	pH 8.0
3[a]	0.02	0.1	nd[b]	5.0[c]	nd
	0.02	0.2	30	1.0	nd
	0.20	0.1	>50[d]	12.0	4.5
5	0.02	0.1	40	8.0	nd
	0.02	0.2	nd	1.1	nd
	0.20	0.1	nd	11.0	nd
	0.20	0.2	nd	4.0	nd
15	0.20	0.1	>50[d]	20.0	nd

[a] Heparin concentrations were based on the average MW of the heparin preparation provided by the manufacturer. Each incubation contained 1.2 μM HTβ-AT. For assay of activity, aliquots from incubations were diluted to a final subunit concentration of 10 nM in 1.0 mM TosGPK-NA, 0.2 M NaCl, 0.1 mg/mL heparin, and 0.1 M Tris-HCl, pH 8.0, at 25 °C. [b] nd = not determined. [c] The $t_{1/2}$ values were determined from fits of time course data (see Figure 8) to an exponential function. Data used for fitting showed at least a 50% loss of activity. [d] Time courses showed <20% loss of activity over 50 h of incubation.

Relatively small affects of pH on the rates of activity loss at 25 °C were amplified at 37 °C (Figure 8 and Table 3). While the higher temperature did not markedly affect the functional stability of HTβ-AT at pH 6.8 (Figure 8A and Table 3), nearly complete loss of activity in 0.2 mM heparin occurred within 50 h at pH 7.5 (Figure 8B, squares) and within 24 h at pH 8.0 (Figure 8C, squares). Time courses for activity loss appeared exponential, and the $t_{1/2}$ values for the decays shown in Figure 8 and other studies not shown are reported in Table 3. Decay rates at pH 7.5 increased upon raising NaCl from 0.1 to 0.2 M or upon lowering heparin from 0.2 to 0.02 mM. They were similar for the 3 and 5 kDa heparins (Figure 8B,D, squares). Increasing the heparin size to 15 kDa only reduced the decay rate by half (Figure 8E). Since heparin concentrations in the incubations were always in excess of the HTβ-AT subunit concentration, activity losses cannot be due to a stoichiometric deficiency in heparin. Rather, it appears that the binding of heparin to HTβ-AT has become weakened at 37 °C above pH 6.8, thus permitting spontaneous inactivation to occur. Further supporting a decrease in the affinity of heparin for HTβ-AT, siHTβ produced in the absence of heparin did not reform active tetramer when incubated with heparin at 37 °C at pH 7.5 (1.5 μM siHTβ, 1.0 mg/mL 3 kDa heparin, 0.1 M NaCl).

Consistent with its stabilizing effect, active tetramer reformation was observed at 37 °C at pH 6.8 (80% recovery; data not shown).

In decays at 37 °C above pH 6.8, IPR-NA activity decreased toward zero activity, but at a rate slightly slower than the TosGPK-NA activity (Figure 8, filled circles). The IPR-NA assay measures the activity of both HTβ-AT and siHTβ-HC with the latter having only 30−40% of the activity of HTβ-AT. Thus, the apparent decrease in the rate of activity loss observed with this assay reflects the production of siHTβ-HC whose activity can only partially compensate for the lost HTβ-AT activity. The loss of all IPR-NA activity upon continued incubation indicates that siHTβ-HC activity also decays at 37 °C. siHTβ-HC activity in incubations can be measured directly as the IPR-NA activity inhibited by BPTI (open circles, plotted relative to IPR-NA activity at time 0). As seen in Figure 8 (panels B−D) BPTI-sensitive activity was not stable and decreased after reaching a level near 20−25% of the HTβ-AT activity at time 0. Thus at 37 °C, spontaneous inactivation leads to an irreversible loss of all HTβ enzymatic activity.

In these studies, siHTβ-HC could have formed in the incubation, and/or upon dilution into the assay, which was at 25 °C and contained heparin. We suggest that siHTβ-HC mostly formed in the assay. Higher temperature likely weakens the interaction of heparin with siHTβ in the same manner as the active tetramer, since both interactions are probably mainly electrostatic in nature (*36*). Hydrolytic activity sensitive to BPTI was not observed when aliquots from incubations were diluted into assay buffer without heparin.

Interaction of siHTβ with the Serpin, α2-AP. Serpins are protein-based protease inhibitors and have not been shown to inhibit HTβ-AT. Unlike tight-binding inhibitors such as BPTI, serpins inhibit activity through a suicide substrate-like mechanism in which the protease cleaves the serpin forming a serpin−acyl-protease complex, which is trapped essentially irreversibly before water hydrolysis of the acyl bond can complete the catalytic cycle (*37*). When analyzed by SDS−PAGE, serpin−protease complexes typically migrate at a size equivalent to the sum of the MWs of the protease and serpin, implying the covalent linkage. In keeping with a suicide substrate, the trapping mechanism is not always 100% efficient, and SDS−PAGE of protease-serpin reactions often shows a band of hydrolyzed-inactivated serpin at a slightly lower MW position than the intact serpin (*37*, *38*). Thus, serpins are expected to react only with dissociated forms of HTβ that have catalytic ability.

The ability of siHTβ/siHTβ-AT (0.6 μM) to react with α2-AP (3.0 μM) was determined in incubations without/with heparin at 25 °C, pH 8.0, as shown in Figure 9A; pH 8.0 permits high concentrations of siHTβ-HC to be generated (see Figure 7). Incubations were monitored using the IPR-NA assay at pH 6.8 (Figure 2). Activity measured for siHTβ is that generated by its conversion to siHTβ-HC upon addition of an aliquot from the incubation to the assay. In the absence of heparin and α2-AP (open circles), the ability of siHTβ to form siHTβ-HC in the assay did not change over the incubation period. Addition of both heparin and α2-AP to the incubation (triangles) resulted in a rapid loss of activity, indicating a reaction between siHTβ-HC and α2-AP. Surprisingly, addition of α2-AP to siHTβ in the absence of heparin reduced the amount of siHTβ-HC activity generated in the assay, suggesting a reaction between α2-AP and siHTβ (Figure 9A, squares). The rate of this activity loss was markedly slower than for siHTβ-HC activity. High MW bands indicative of covalent complexes between α2-AP (70 kDa) and both siHTβ and siHTβ-HC were observed in SDS−PAGE analyses of aliquots from incubations (Figure 10A). Consistent with the different rates of activity loss in Figure 9A, bands indicative of protease−serpin complexes appeared more rapidly in incubations containing heparin than without heparin. In lanes where complexes were detected, bands migrating slightly faster than intact α2-AP also were seen, indicative of enzymatic turnover and inactivation of α2-AP. These results demonstrate that both siHTβ and siHTβ-HC react with serpins, forming both the covalent complex and hydrolyzed serpin.

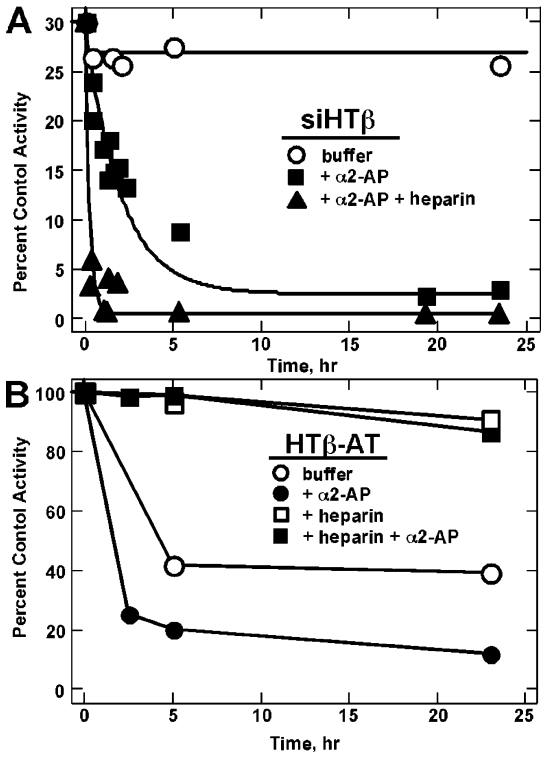

FIGURE 9: Reaction of siHTβ and HTβ-AT with α2-AP. 0.6 μM siHTβ subunits (A) or 1.0 μM HTβ-AT subunits (B) were incubated with 3.0 μM α2-AP ± 1.0 mg/mL heparin at 25 °C in 0.1 M NaCl and 0.1 M Tris, pH 8.0. Activities were measured using pH 6.8 assay conditions for IPR-NA in Figure 2. Measurements were made on aliquots from incubations diluted to a final subunit concentration of 10 nM in assay medium, which effectively stopped further reaction with the serpin during the assay. siHTβ activity in panel A (open circles) results from its interaction with heparin in the assay. The percent control activities in panel A were calculated relative to the activity of the heparin-stabilized HTβ-AT control (100%) in panel B (open squares). The curved lines in panel A are single exponentials fit to the data.

The reaction of free and heparin-stabilized HTβ-AT (1.0 μM subunits) with α2-AP (3.0 μM) also was evaluated using the same incubation/assay conditions as above. As shown in Figures 9B and 10B, HTβ-AT incubated with α2-AP in the presence of heparin (closed squares) for up to 24 h lost little, if any, activity relative to a stabilized control (open squares) and showed very little covalent complex by SDS−PAGE. In the absence of heparin (open circles), HTβ-AT lost activity due to spontaneous inactivation, the plateau at 40% activity reflecting conversion of siHTβ to siHTβ-HC

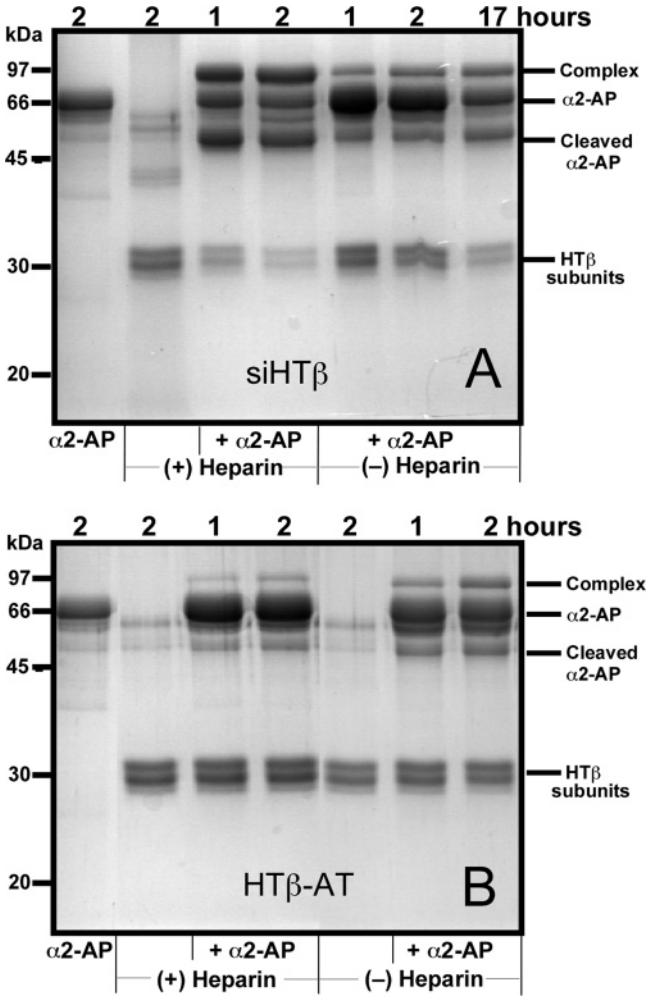

FIGURE 10: SDS−PAGE analyses of reactions of α2-AP with siHTβ and HTβ-AT. Reaction conditions were similar to those used in Figure 9. Reactions were terminated by addition of hot SDS−DTT. Lanes 1 in panels A and B are controls containing 3.0 μg of α2-AP alone. All other lanes contained the equivalent of 1.0 μg of protease (siHTβ in panel A and HTβ-AT/siHTβ in panel B) with or without 6.0 μg of α2-AP. In the absence of heparin, HTβ-AT will undergo spontaneous inactivation resulting in formation of siHTβ; therefore, the right-hand side of panel B is similar to the results for siHTβ in the absence of heparin in panel A.

in the assay. A similar incubation with α2-AP produced more than a 40% loss in activity (compare open and closed circles), consistent with a reaction between α2-AP and siHTβ produced during spontaneous inactivation. A band consistent with a covalent complex between α2-AP and siHTβ was observed by SDS−PAGE (Figure 10B). These studies show that heparin-stabilized HTβ-AT does not spontaneously dissociate to active subunits and that the HTβ species capable of reacting with serpins are siHTβ and siHTβ-HC.

The reactivity of α2-AP is not dependent upon heparin as is, e.g., antithrombin III (*37*); therefore, the difference in the rates of reaction of α2-AP with siHTβ and siHTβ-HC in Figure 10A likely reflects the different catalytic abilities of each siHTβ form. To quantify this difference, k_{assoc} for the reactions were determined. For the reaction of α2-AP with siHTβ (Figure 9A, squares), k_{obs} was determined by fitting the data to a single -exponential decay which yielded an apparent k_{assoc} of 30 M^{-1} s^{-1}. The rate of α2-AP inhibition of siHTβ-HC (Figure 9A, triangles) was too fast for reliable fitting as a single exponential. However, since siHTβ-HC hydrolyzes peptide-NA substrates, k_{assoc} could be determined using the progress curve method described in Experimental Procedures (*27*). The average k_{assoc} value for two determinations at different inhibitor concentrations (1.3 and 2.5 μM) was 2140 ± 130 M^{-1} s^{-1} (Figure S2, Supporting Information). Thus, the reaction with α2-AP with siHTβ-HC was 71-fold faster than with siHTβ.

DISCUSSION

This study reconciles reports of a catalytically competent monomeric form of HTβ (*18*, *21*−25) with our previous findings on the structural and catalytic properties of HTβ and its spontaneous inactivation under near physiological conditions. On the basis of our studies as summarized in the introduction and Figure 1, a monomeric form can arise only by dissociation of the inactive-destabilized tetramer formed during spontaneous inactivation (*5*, *9*, *10*). Such monomers would be inactive and therefore require structural perturbation to exhibit activity. This work establishes the conditions that can produce such structural change, the enzymatic properties of the resulting catalytic forms, and their relationship to the active tetramer. Moreover, the results provide insight into the active site structure of monomer and tetramer catalytic forms along with the physiological relevance of such species and can account for monomeric forms described by others (*18*, *21*−25).

Interaction with Serpins Identifies Two Catalytic Forms Other than the Tetramer. Serpins are proteins that irreversibly inhibit proteases by a suicide substrate-like mechanism that requires proteolytic cleavage to activate the serpin (*37*). The position of the active sites in HTβ-AT appears to preclude their interaction with protein-based inhibitors such as serpins. In this study we show that the active tetramer, HTβ-AT, in the presence of heparin did not react with α2-AP even at pH 8.0, a condition suggested to produce direct dissociation to active monomers (*21*). However, a covalent complex characteristic of serpin inhibition as well as hydrolyzed-inactive serpin was observed with the products of spontaneous inactivation (siHTβ) in both the absence and the presence of heparin. The reaction rate in the presence of heparin was much higher (k_{assoc} 2100 M^{-1} s^{-1}) than in its absence (k_{assoc} 30 M^{-1} s^{-1}), consistent with activation of siHTβ upon interaction with heparin to form a new species, siHTβ-HC. k_{assoc} values for the reaction of siHTβ/siHTβ-HC with α2-AP were much less than those (approximately 10^7 M^{-1} s^{-1}) reported for other proteases (*39*), suggesting that both siHTβ species are not true targets for this serpin.

The reaction of α2-AP with siHTβ in the absence of heparin is the first evidence that this species, which does not hydrolyze model peptide-NA substrates, has hydrolytic potential, albeit limited. Serpins being large proteins (α2-AP = 70 kDa) are capable of more extensive noncovalent interactions with siHTβ than a peptide substrate. Thus, we suggest that such noncovalent interactions provide the free energy needed to reorganize the active site of siHTβ to a conformation that is more hydrolytic. This phenomenon is in essence an induced-fit activation of an intrinsically inactive siHTβ. Fibrinogen, a protein hydrolyzed by HTβ-AT (*33*−*35*) and siHTβ-HC (*21*, *25*), was not hydrolyzed by siHTβ, perhaps indicating the highly specific nature of the reaction with α2-AP.

Formation and Enzymatic Properties of siHTβ-HC. The species siHTβ-HC produced by addition of heparin to dilute siHTβ not only reacted with α2-AP much faster than siHTβ but also hydrolyzed peptide-NA substrates and fibrinogen. Formation of siHTβ-HC was dependent on heparin concentration as rates of peptide-NA hydrolysis increased to a maximal rate with increasing heparin concentration (Figures 3 and 4). Similar activation also was observed using other highly charged polysaccharides, dextran sulfate and dermatan sulfate (Figure 4). Maximal activities obtained with different polysaccharides were similar, although the concentration dependencies differed. The saturable nature of the concentration dependence and similar maximal rates with different polysaccharides showed that the complex between siHTβ and charged polysaccharides is both well-defined and the catalytic species. This fundamental understanding of the activation process allowed us to establish the catalytic properties of the active monomer with more clarity and detail than in other studies (*18*, *21*−*25*) and permitted a meaningful comparison of these properties with those of HTβ-AT.

Under conditions that produce maximal activity, both siHTβ-HC and HTβ-AT hydrolyzed a series of peptide substrates with the same order of preference (Table S1, Supporting Information), but with markedly different catalytic properties. HTβ-AT activity was unaffected by heparin (Figure 3), increased with pH reaching a maximum level near 8.5 (Figure 5), and was relatively unaffected by a change in the NaCl concentration of assays. In contrast, siHTβ-HC activity was highly dependent on heparin and NaCl concentrations (Figures 2−5 and Table 1) and demonstrated a bell-shaped pH activity profile with highest activity between pH 6.8 and pH 7.5 (Figure 5). Moreover, siHTβ-HC was less catalytic than HTβ-AT even when saturated with substrate (Table 2) and especially at pH >7.0, a region where serine proteases typically function most efficiently (Figures 3 and 5). Thus, siHTβ-HC is a distinct enzymatic species with similar substrate preferences but much less catalytic ability than a subunit within the tetramer.

Heparin Interaction with HTβ-AT Limits siHTβ-HC Formation. Formation of siHTβ-HC was limited to low siHTβ concentrations because high protein concentrations favor reassembly of the active tetramer (Figure 7). These findings indicate that heparin binds more strongly to the active tetramer than to the monomeric siHTβ and are consistent with the virtually complete stability of heparin−HTβ-AT at 25 °C as well as with our arguments that the tetramer is the favored catalytic species. The model in Figure 1 accounts for such findings. The irreversible nature of the interaction between heparin and HTβ-AT implies a strong interaction (step 5) that can drive the equilibrium between the various dissociated forms derived from spontaneous inactivation toward the active tetramer (curved arrow). Active monomer is a consequence of step 2, the equilibrium governing dissociation of the inactive-destabilized tetramer. As the result of this step, the thermodynamics and kinetics for reassembly of the active tetramer will become more unfavorable as the siHTβ concentration decreases, eventually reaching a point where siHTβ cannot reform tetramer even though it can bind heparin. The minimum siHTβ concentration required for tetramer formation was lower at pH 6.0 than at pH 8.0. Thus, in contrast to that reported in other studies (*24*, *25*), high rather than low pH permits higher concentrations of the catalytic monomer.

Above pH 6.8, the functional stability of HTβ-AT in the presence of excess heparin decreased dramatically at 37 °C, demonstrating that step 5 in Figure 1 had become reversible, thus permitting spontaneous inactivation to occur. Varying the size of heparin used in incubations at 37 °C from 3 to 15 kDa did not markedly affect the rate of HTβ-AT activity loss. At 37 °C activity consistent with the formation of siHTβ-HC increased with loss of HTβ-AT activity; however, upon continued incubation all catalytic activity was irreversibly lost. The inability of heparin to maintain HTβ-AT or siHTβ-HC activity at 37 °C is consistent with a weakened binding to both species. Such behavior is expected for an interaction dominated by electrostatic forces. Thus, at 37 °C above pH 6.8, spontaneous inactivation leads to irreversible inactivation of all species.

Reduced stability of the active tetramer in the presence of heparin at 37 °C, pH 7.5, has been noted by others, but decay rates have been inconsistent. Alter et al. (*19*) using heparin (1.0−5.0 μM, 0.2 μM subunits, 0.12 M NaCl) at about a 20−200-fold lower concentration than in our study showed inactivation of HTβ-AT in the presence 4 and 6 kDa heparins but no change in activity with heparin of larger size (12−20 kDa). Their decay rates with low MW heparins were slower than expected from our data. However, incubations were only monitored for 2 h and were not complete, making their calculation of rate constants subject to greater error than in our studies. On the other hand, Hallgren et al. (*23*) using a very low concentration of heparin (1.0 nM heparin, ≤0.15 nM subunits, 0.15 M NaCl, estimated from their report) showed inactivation of HTβ-AT in the presence of 15 kDa heparin at a rate much faster than in our study (70−80% loss by 20 min). A faster rate agrees with our premise of weakened binding, since lower heparin concentrations would produce less saturation of HTβ-AT, which in turn would hasten the rate of spontaneous inactivation.

Structural Properties of siHTβ-HC. In our model of spontaneous inactivation (Figure 1), concerted conformational changes within the active site and interface regions lead to both activity loss and tetramer dissociation (*5*, *9*, *10*, *15*). Tight binding of heparin to each of the subunits within the tetramer prevents these conformational changes by stabilizing the structure of each subunit in a fashion similar to the structural stabilization that sometimes occurs upon binding a ligand to a protein. Our studies showing that small competitive inhibitors that interact mainly with the primary substrate binding pocket can both stabilize the tetramer and mediate reformation of the active tetramer support such a mechanism for the influence of heparin (*10*). The cross-linking of subunits by heparin across the smaller of the two types of interfaces that form the tetramer, as depicted in step 5 of Figure 1, has been proposed from modeling studies (*40*, *41*) and also has been suggested to be the basis for heparin stabilization of the active tetramer. In this model heparin binding enhances the strength of presumably weak intersubunit contacts based mainly on nonspecific hydrophobic effects (*40*, *41*). This cross-linking model, in contrast to our model, allows direct dissociation of the tetramer to active monomers, which then inactivate. We believe our model more readily explains the formation and properties of siHTβ-HC.

We suggest that heparin binds to monomeric siHTβ, possibly at the same site that exists on a subunit within the tetramer, and this interaction restores some activity by driving a conformational change that brings the structure of the monomer closer to, but not identical with, that of a subunit within the active tetramer. The catalytic ability of the monomer is less than that of a subunit within the tetramer because additional conformational changes associated with tetramer reassembly are required to fully form the active site. In the cross-linking model, it is harder to rationalize heparin stabilizing an active monomer, since the role of heparin is to prevent dissociation of weakly bound subunits; moreover, such a monomer would be expected to have catalytic properties more comparable with a subunit within the tetramer.

On the basis of the crystal structures of HTβ-AT (*7*, *40*) and closely related structures (*41*, *42*), the active sites in the tetramer are intimately associated with the larger of the two types of interfaces between subunits such that the active site structure of each subunit includes residues from the neighboring subunit. This arrangement precludes full duplication of the active site as found in the tetramer by a monomeric form. Lastly, the computer modeling discussed above places the heparin binding sites along the peripheral surfaces of the subunits in the vicinity of the small interface and therefore remote from the active site (*40*, *41*). Thus, heparin is predicted to have no direct interactions with residues forming the active site in the tetramer. Our studies showing that the hydrolytic activity of the tetramer was not affected by heparin are consistent with such a remote binding site.

The effect of pH on the hydrolytic activities of HTβ-AT and siHTβ-HC was very different (Figure 5). HTβ-AT activity increased with pH to a maximum level, whereas siHTβ-HC exhibited a bell-shaped activity profile with a maximum between pH 6.8 and pH 7.5. For both HTβ species, the activity increase with pH over the low pH range is likely related, at least in part, to the expected titration of His57 of the catalytic triad (*31*, *32*, *43*). The decrease in siHTβ-HC activity in the alkaline pH range may be related to a buried ionic bond between the α-amino group of Ile16 and the carboxylate of Asp194. This ionic bond is a conserved structural feature of serine proteases (*43*−*45*) including HTβ-AT (*7*, *41*, *42*), which we previously have suggested is disrupted during spontaneous inactivation (*5*, *9*, *10*, *15*).

A bell-shaped activity profile similar to that in Figure 5 is seen for chymotrypsin activity measured under conditions with $[S]_0 < K_m$ (*46*−*48*). This decrease in activity at high pH was attributed to disruption of the Ile16−Asp194 salt bridge by titration of the α-amino group of Ile16. The Ile16−Asp194 salt bridge is formed during activation of a serine protease from its zymogen and functions to stabilize the S1 pocket in a conformation optimal for the recognition and catalysis of substrates (*43*−*45*). Although the pK_a of a free α-amino group is about 8, in many serine proteases structural stabilization provided by the protein permits maximal activity well into the alkaline pH range by increasing the apparent pK_a of the α-amino group (*43*, *47*, *48*). Thus, while the pH profile for HTβ-AT in Figure 5 is common for many serine proteases, the profile for siHTβ-HC is consistent with an Ile16−Asp194 salt bridge minimally stabilized by protein structure. The crystal structure of HTβ-AT finds the Ile16−Asp194 salt bridge near the small subunit interface (*7*, *40*), suggesting that it could become less stable after spontaneous inactivation. These arguments suggest that activation of siHTβ by heparin binding can be explained, at least in part, by a conformational change permitting the formation of a weakened Ile16−Asp194 salt bridge.

Our measurement of an apparent K_d for the interaction of heparin with siHTβ provides the first direct evidence for a discrete heparin binding site on HTβ. Measurements of K_d showed that heparin binding to siHTβ was stronger at low than high pH. Although not quantified, a similar pH effect was observed for both heparin stabilization of HTβ-AT and heparin-mediated reassembly of the active tetramer. The Ile16−Asp194 salt bridge could contribute to these pH dependencies since stabilization/formation of this bond would be less favorable at high than low pH due to the deprotonation of the α-amino group of Ile16. Mutational studies also have implicated a series of surface His residues (pK_a 6.0), which may play a role in the observed pH dependencies (*49*).

Model Incorporating Catalytically Active siHTβ Species. The model in Figure 1 accounts for the formation and interrelationships of the various species that can be derived from HTβ. Conversion of HTβ-AT to the inactive-destabilized tetramer by spontaneous inactivation (step 1), dissociation of the inactive-destabilized tetramer (step 2), and stabilization of HTβ-AT by interaction with heparin (step 5) and competitive inhibitors (step 6) have been discussed here and in the introduction. Steps 3 and 4 are added to account for the properties of the active monomeric forms of siHTβ just described.

The conformational change in step 3 was introduced to account for the reaction of siHTβ with the inhibitor α2-AP, while not being able to hydrolyze peptide-NA substrates. We speculate that highly specific noncovalent interactions with inhibitor are driving its hydrolysis by siHTβ through an induced-fit mechanism. Thus, the active species is likely only a small fraction of the total siHTβ population as depicted by the equilibrium lying far toward the inactive state.

Step 4 accounts for the interaction of heparin with monomeric siHTβ to form a complex, siHTβ-HC, that reacts with α2-AP much faster than siHTβ and can now hydrolyze peptide-NA substrates and fibrinogen. While the substrate specificity of siHTβ-HC was similar to that of HTβ-AT, the hydrolytic properties of each species were distinct, indicating that siHTβ-HC is not equivalent to a subunit within the tetramer but rather a unique species with less catalytic potential. Given the structural observations discussed above, we depict siHTβ-HC with the S1 pocket and Ile16−Asp194 salt bridge somewhat different compared to their state in the subunit. The irreversible nature of the interaction between heparin and HTβ-AT at 25 °C indicates that a direct equilibrium will not exist between siHTβ-HC and the heparin-stabilized tetramer and that the only pathway leading to active monomer is through spontaneous inactivation. The large curved arrow emphasizes that formation of siHTβ-HC is limited to low siHTβ concentrations where thermodynamic/kinetic concerns preclude reassociation of subunits.

At 37 °C above pH 6.8, the interaction of heparin with HTβ-AT weakens sufficiently so that step 5 becomes reversible, even when the heparin concentration is in vast excess of HTβ. This reversibility allows spontaneous inactivation to proceed. siHTβ produced by spontaneous inactivation of HTβ-AT in the presence of excess heparin would

be in equilibrium with siHTβ-HC (step 4), although at 37 °C, the K_d for heparin binding to siHTβ has likely increased from its value at 25 °C. The existence of siHTβ/siHTβ-HC is transient as prolonged incubation at 37 °C leads to a new step (not shown) producing irreversible inactivation of siHTβ.

Unifying Other Reports of HTβ Catalytic Monomers with Our Model. Addington and Johnson (*18*) were the first to report a monomeric species with activity. They showed that HTβ-AT inactivated by incubation in low salt at 37 °C eluted during SEC as a minor tetramer peak and major monomer peak. The monomer peak had a small amount of activity toward the substrate Z-Lys-SBzl at pH 7.5 which increased when heparin (0.5 mg/mL) was added to the assay. While a protein-based inhibitor was not used to rule out reformation of the active tetramer during the assay, our studies suggest that the protein concentrations in these studies would be too low to permit reassembly. Thus, the measured activity was likely from an active monomer produced by step 4 in our model.

In a series of studies, Schwartz and colleagues (*20*, *24*, *25*) described highly divergent properties for HTβ at pH 6.0 and 7.5. They reported that the inactivation of HTβ-AT at pH 7.5 (25 °C) in the absence of heparin was irreversible and that heparin-mediated reformation of the active tetramer from inactivated HTβ occurs only at pH 6.0. In very early work, they had reported reformation of the active tetramer at pH 6.0 in the absence of heparin. However, this finding appears superseded by their identification of a catalytic monomer active only in the presence of heparin at pH 6.0. The catalytic monomer was postulated to be an intermediate that makes reformation of the active tetramer possible at low pH.

The divergent properties reported for HTβ at low and high pH were primarily based on studies where heparin activation of siHTβ and reformation of the active tetramer were each evaluated using only a single set of conditions. Our studies show that the interaction of heparin with siHTβ leading to formation of siHTβ-HC or active tetramer is dependent on many variables: siHTβ concentration, heparin concentration, ionic strength, pH, and temperature. On the basis of our data, the single set of experimental conditions (about 10 nM siHTβ, 25 μg/mL heparin, and approximately 0.1 M NaCl/KCl) used by Schwartz and colleagues would have produced a catalytic monomer at low pH where the K_d for heparin binding is lowest but would have been unlikely to produce this catalytic monomer at higher pH where the K_d is higher. On the basis of our measurements of maximal activities, the catalytic monomer is most active near neutral pH.

Analogously, the low siHTβ concentration (0.1 μM siHTβ) used by Schwartz and colleagues (*20*, *24*) to characterize tetramer reformation at 25 °C would have only produced reassembly at low pH where the concentration of siHTβ needed to drive tetramer reformation is lowest (Figure 7). The favorable impact of low pH on the heparin stabilization of HTβ-AT and tetramer reassembly as shown in our study and evident in the work of Schwartz and colleagues (*20*, *24*) makes a greater difference at 37 °C. At this temperature, low pH favors stabilization of the active tetramer by heparin whereas above pH 6.8 heparin binding weakens dramatically, permitting spontaneous inactivation as an essentially irreversible process. Thus, our results permit us to incorporate the results of Schwartz and colleagues (*20*, *24*) into the modified version of our previous description of spontaneous inactivation (Figure 1).

Fajardo et al. (*21*) suggested that a catalytic monomer could be produced by direct dissociation of the heparin-stabilized tetramer at pH 7.5. Their data are difficult to reconcile with ours because they do not define a form of HTβ comparable to siHTβ. For instance, in their SEC studies to distinguish monomer and tetramer species, the active tetramer was first incubated at 37 °C for 30 min in the absence or presence of very low concentrations of heparin. Then SEC was preformed at 25 °C on a column equilibrated at pH 6.0 with 10 μM heparin (30 or 75 μg/mL depending on size). Column fractions were assayed using IPR-NA at pH 6.0. We suggest that the incubation at 37 °C produced siHTβ and SEC at low pH in heparin led to some tetramer reformation, yielding the mixture of species resolved on their columns. Because HTβ-AT and siHTβ-HC would have nearly the same activity under their assay conditions (pH 6.0; see Figure 5), their column profiles with different proportions of monomer and tetramer would appear to have similar total activities. This may have led the authors to suggest the direct dissociation of active tetramer in the presence of heparin. siHTβ-HC as defined by our studies appears to correspond to the catalytic monomer described by Fajardo et al. (*21*). Their catalytic monomer degraded fibrinogen and fibronectin, whereas the active tetramer only degraded fibrinogen. In Figure 6, we show degradation of fibrinogen by siHTβ-HC at pH 6.8, and we have confirmed the selectivity for fibronectin hydrolysis (data not shown).

Strik et al. (*22*) have described a covalent complex between SerpinB6 and HTβ in cell lysates of HMC-1 cells, a continuous line of mast cells. This complex did not form in cell lysates made in high salt, suggesting that inactivation/dissociation of the active tetramer must occur prior to reaction with the serpin. Our data support their findings by showing that spontaneous inactivation is required to produce HTβ species capable of interacting with the serpin, α2-AP.

Is siHTβ Enzymatic Activity Physiologically Relevant? In this study, we show that the only pathway for dissociation of tetrameric HTβ at 25 °C (Figure 1) or 37 °C is through spontaneous inactivation and that siHTβ-HC, the catalytic monomer described in this study, is the only monomeric form of HTβ capable of hydrolyzing both peptides and proteins. It is generally assumed that HTβ is stored within the mast cell complexed to heparin proteoglycans and that this complex is secreted into the extracellular space during mast cell degranulation. The pH of a mast cell granule has been reported to be 5.5 (*50*), which would stabilize HTβ-AT−heparin complexes within granules even at 37 °C (Figure 8). Upon secretion, HTβ-AT−heparin complexes will encounter higher pH and become diluted. At 37 °C a marked change in the stability of HTβ-AT occurs between pH 6.8 and pH 7.5 (Figure 8 and Table 3). If, as expected, the extracellular pH is closer to 7.5, secreted HTβ-AT−heparin complexes will readily dissociate, and activity will be lost by spontaneous inactivation (*17*, *19*). Since heparin-free HTβ-AT decays at 37 °C with a half-life of approximately 1 min (*17*, *19*), loss of activity could be extremely fast if the local environment is devoid of free heparin. Free heparin in the extracellular environment is likely to be low due to dilution during diffusion away from the site of release,

competition from the presence of other mast cell proteases (chymase, cathepsin G, carboxypeptidase) that bind heparin (*51*, *52*), and competition from an influx of blood proteins (e.g., antithrombin III, lactoferrin), many of which also bind heparin (*16*, *53*).

A temperature of 37 °C and low heparin concentration in the extracellular environment also would not favor formation of siHTβ-HC; thus we predict that the spontaneous inactivation of secreted HTβ-AT will not lead to generation of the catalytic monomer in vivo. It is unlikely that other GAGs in the extracellular space would bind to siHTβ, since these GAGS are less charged per dissacharride unit and, as shown in this study, bind more weakly to siHTβ than does heparin (Table 1 and Figure 4). What cannot be completely discounted is the presence in the extracellular space of a specific macromolecular substrate that could induce siHTβ activity in a manner similar to the induced-fit mechanism we have suggested for α2-AP. The interaction and hydrolysis of gelatin by monomeric HTβ recently described may be an instance of such a biological substrate (*29*).

We found little difference in the rates of activity loss at 37 °C with heparins of sizes ranging from 3 to 15 kDa, suggesting that the size of heparin will not greatly affect activity loss rates, at least at 37 °C. However, in vivo, heparin is stored as a proteoglycan in which multiple heparin chains are linked to a single polypeptide chain. A study that monitored HTβ activity after disruption of isolated mast cells showed loss of activity with time (*54*), indicating HTβ-AT bound to native heparin−proteoglycans was not stable at 37 °C. Thus, temperature and pH are probably the major factors determining the functional lifetime of HTβ-AT in the extracellular environment.

In summary, we show that monomeric species with catalytic activity are derived from the products of spontaneous inactivation, siHTβ, and are significantly less catalytic than a subunit within the tetramer. The ability of anionic polysaccharides to bind to dilute siHTβ at 25 °C and to produce a complex of marginal activity is likely a consequence of a high-affinity heparin binding site on the monomer and to low protein concentrations where thermodynamics/kinetics for tetramer reassembly are unfavorable. The inability to form a polysaccharide−siHTβ complex with activity equal to a subunit within the tetramer argues that interactions between subunits are required for optimal catalytic activity and that the tetramer is the physiologically relevant catalytic species. At 37 °C, the apparent weakened binding of heparin to HTβ-AT and likely siHTβ suggests a much less important role for heparin in the regulation of HTβ catalytic activity in vivo than has been implied by in vitro studies at 25 °C. Taken together, our results remain compatible with our earlier suggestion that spontaneous inactivation of HTβ-AT functions as an autoregulatory process that replaces inhibition by a protein-based inhibitor.

ACKNOWLEDGMENT

Recombinant HTβ used in this study was expressed at the Recombinant Vector and Protein Expression Facility, Wistar Institute, Philadelphia, PA.

SUPPORTING INFORMATION AVAILABLE

Table S1 comparing the effect of pH and NaCl concentration on HTβ-AT and siHTβ-HC hydrolysis of five model nitroanilide substrates, Figure S1 showing the differential effect of BPTI on the hydrolysis of fibrinogen by siHTβ-HC and HTβ-AT, and Figure S2 showing the progress curves used to determine k_{assoc} for α2-AP inhibition of siHTβ-HC. This material is available free of charge via the Internet at http://pubs.acs.org.

REFERENCES

1. Schwartz, L. B., Irani, A.-M. A., Roller, K., Castells, M. C., and Schechter, N. M. (1987) Quantitation of histamine, tryptase, and chymase in dispersed human T and TC mast cells, *J. Immunol. 138*, 2611−2615.
2. Schwartz, L. B. (1994) Tryptase: a mast cell serine proteinase, *Methods Enzymol. 244*, 88−100.
3. Schwartz, L. B., and Bradford, T. R. (1986) Regulation of tryptase from lung mast cells by heparin: stabilization of the active tetramer, *J. Biol. Chem. 261*, 7372−7379.
4. Smith, T. J., Houghland, M. W., and Johnson, D. A. (1984) Human lung tryptase: purification and characterization, *J. Biol. Chem. 259*, 11046−11051.
5. Schechter, N. M., Eng, G. Y., Selwood, T., and McCaslin, D. R. (1995) Structural changes associated with the spontaneous inactivation of the serine proteinase human tryptase, *Biochemistry 34*, 10628−10638.
6. Niles, A., Maffitt, M., Haak-Frendscho, M., Wheeless, C. J., and Johnson, D. A. (1998) Recombinant human mast cell tryptase: stable expression in *Pichia pastoris* and purification of fully active enzyme, *Biotechnol. Appl. Biochem. 28*, 125−131.
7. Pereira, P. J. B., Bergner, A., Macedo-Ribeiro, S., Huber, R., Matschiner, G., Fritz, H., Sommerhoff, C. P., and Bode, W. (1998) Human β-tryptase is a ring-like tetramer with active sites facing a central pore, *Nature 392*, 306−311.
8. Chan, H., Elrod, K. C., Numerof, R. P., Sideris, S., and Clark, J. M. (1999) Expression and characterization of recombinant mast cell tryptase, *Protein Expression Purif. 15*, 251−257.
9. Selwood, T., Wang, Z.-M., McCaslin, D. R., and Schechter, N. M. (2002) Diverse stability and catalytic properties of human tryptase α and β isoforms are mediated by residue differences at the S1 pocket, *Biochemistry 41*, 3329−3340.
10. Selwood, T., Smolensky, H., McCaslin, D. R., and Schechter, N. M. (2005) The interaction of human tryptase-β with small molecule inhibitors provides new insights into the unusual functional instability and quaternary structure of the protease, *Biochemistry 44*, 3580−3590.
11. Cromlish, J. A., Seidah, N. G., Marcinkiewicz, M., Hamelin, J., Johnson, D. A., and Chrétien, M. (1987) Human pituitary tryptase: molecular forms, NH_2-terminal sequence, immunocytochemical localization, and specificity with prohormone and fluorogenic substrates, *J. Biol. Chem. 262*, 1363−1373.
12. Tanaka, T., McRae, B. J., Cho, K., Cook, R., Fräki, J. E., Johnson, D. A., and Powers, J. C. (1983) Mammalian tissue trypsin-like enzymes: comparative reactivities of human skin tryptase, human lung tryptase, and bovine trypsin with peptide 4-nitroanilide and thioester substrates, *J. Biol. Chem. 258*, 13552−13557.
13. Harvima, I. T., Schechter, N. M., Harvima, R. J., and Fräki, J. E. (1988) Human skin tryptase: purification, partial characterization and comparison with human lung tryptase, *Biochim. Biophys. Acta 957*, 71−80.
14. Caughey, G. H., Raymond, W. W., Bacci, E., Lombardy, R. J., and Tidwell, R. R. (1993) Bis(5-amidino-2-benzimadazolyl)-methane and related amidines are potent, reversible inhibitors of mast cell tryptases, *J. Pharmacol. Exp. Ther. 264*, 676−682.
15. Selwood, T., McCaslin, D. R., and Schechter, N. M. (1998) Spontaneous inactivation of human tryptase involves conformational changes consistent with conversion of the active site to a zymogen-like structure, *Biochemistry 37*, 13174−13183.
16. Alter, S. C., Kramps, J. A., Janoff, A., and Schwartz, L. B. (1990) Interactions of human mast cell tryptase with biological protease inhibitors, *Arch. Biochem. Biophys. 276*, 26−31.
17. Schechter, N. M., Eng, G. Y., and McCaslin, D. R. (1993) Human skin tryptase: kinetic characterization of its spontaneous inactivation, *Biochemistry 32*, 2617−2625.
18. Addington, A. K., and Johnson, D. A. (1996) Inactivation of human lung tryptase: evidence for a re-activatable tetrameric intermediate and active monomers, *Biochemistry 35*, 13511−13518.

19. Alter, S. C., Metcalfe, D. D., Bradford, T. R., and Schwartz, L. B. (1987) Regulation of human mast cell tryptase: effects of enzyme concentration, ionic strength and negative charge density, *Biochem. J. 248*, 821−827.
20. Ren, S., Sakai, K., and Schwartz, L. B. (1998) Regulation of human mast cell β-tryptase: conversion of inactive monomer to active tetramer at acid pH, *J. Immunol. 1998*, 4561−4569.
21. Fajardo, I., and Pejler, G. (2003) Formation of active monomers from tetrameric human β-tryptase, *Biochem. J. 369*, 603−610.
22. Strik, M. C. M., Wolbink, A., Wouters, D., Bladergroen, B. A., Verlaan, A. R., van Houdt, I. S., Hijlkema, S., Hack, C. E., and Kummer, J. A. (2004) Intracellular serpin serpinB6 (PI6) is abundantly expressed in human mast cells and forms complexes with beta-tryptase monomers, *Blood 103*, 2710−2717.
23. Hallgren, J., Lindahl, S., and Pejler, G. (2005) Structural requirements and mechanism for heparin-dependent activation of tetramerization of human βI and βII tryptase, *J. Mol. Biol. 345*, 129−139.
24. Fukuoka, Y., and Schwartz, L. B. (2004) Human β-tryptase: detection and characterization of the active monomer and prevention of tetramer reconstitution by protease inhibitors, *Biochemistry 43*, 10757−10764.
25. Fukuoka, Y., and Schwartz, L. B. (2006) The B12 anti-tryptase monoclonal antibody disrupts the tetrameric structure of heparin-stabilized β tryptase to from monomers that are inactive at nuetral pH and active at acidic pH, *J. Immunol. 176*, 3165−3172.
26. Wang, Z.-M., Walter, M., Selwood, T., Rubin, H., and Schechter, N. M. (1998) Recombinant expression of human mast cell proteases chymase and tryptase, *Biol. Chem. 379*, 167−174.
27. Morrison, J. F., and Walsh, C. T. (1987) The significance of slow-binding enzyme inhibitors, *Adv. Enzymol. 61*, 210−301.
28. Laemmli, U. K. (1970) Cleavage of structural proteins during the assembly of the head of bacteriophage T4, *Nature 227*, 680−685.
29. Fajardo, I., and Pejler, G. (2003) Human mast cell β-tryptase is a gelatinase, *J. Immunol. 171*, 1493−1499.
30. Hedstrom, L. (2002) Serine protease mechanism and specificity, *Chem. Rev. 102*, 4501−4523.
31. Perona, J. J., and Craik, C. S. (1995) Structural basis of substrate specificity in the serine proteases, *Protein Sci. 4*, 337−360.
32. Polgar, L. (1989) *Mechanism of protease action*, CRC Press, Boca Raton, FL.
33. Schwartz, L. B., Bradford, T. R., Littman, B. H., and Wintroub, B. U. (1985) The fibrinogenolytic activity of purified tryptase from human lung mast cells, *J. Immunol. 135*, 2762−2767.
34. Ren, S., Lawson, A. E., Carr, M., Baumgarten, C. M., and Schwartz, L. B. (1997) Human tryptase fibrinogenolysis is optimal at acidic pH and generates anticoagulent fragments in the presence of the anti-tryptase monoclonal antibody B12, *J. Immunol. 159*, 3540−3548.
35. Thomas, V. A., Wheeless, C. J., Stack, M. S., and Johnson, D. A. (1998) Human mast cell tryptase fibrinogenolysis: kinetics, anticoagulation mechanism, and cell adhesion disruption, *Biochemistry 37*, 2291−2298.
36. Muñoz, E. M., and Linhardt, R. J. (2004) Heparin-binding domains in vascular biology, *Arterioscler., Thromb., Vasc. Biol. 24*, 1549−1557.
37. Gettins, P. G. W. (2002) Serpin structure, mechanism, and function, *Chem. Rev. 102*, 4751−4803.
38. Schechter, N. M., Jordan, L. M., James, A. M., Cooperman, B. S., Wang, Z.-m., and Rubin, H. (1993) Reaction of human chymase with reactive site variants of α1-antichymotrypsin: modulation of inhibitor vs substrate properties, *J. Biol. Chem. 268*, 23626−23633.
39. Holmes, E. W., Lijnen, H. R., and Collen, D. (1987) Characterization of recombinant human α2-antiplasmin and of mutants obtained by site-directed mutagenesis of the reactive site, *Biochemistry 26*, 5133−5140.
40. Sommerhoff, C. P., Bode, W., Pereira, P. J., Stubbs, M. T., Sturzebecher, J., Piechottka, G. P., Matschiner, G., and Bergner, A. (1999) The structure of the human βII-tryptase tetramer: fo-(u)r better or worse, *Proc. Natl. Acad. Sci. U.S.A. 96*, 10984−10991.
41. Marquardt, U., Zettl, F., Huber, R., Bode, W., and Sommerhoff, C. (2002) The crystal structure of human α1-tryptase reveals a blocked substrate-binding region, *J. Mol. Biol. 321*, 491−502.
42. Rohr, K. B., Selwood, T., Marquardt, C., Huber, H., Schechter, N. M., Bode, W., and Than, M. E. (2006) X-ray structures of free and leupeptin-complexed human α1-tryptase mutants: indication for an alpha to beta-tryptase transition, *J. Mol. Biol. 357*, 195−209.
43. Hedstrom, L., Lin, T.-Y., and Fast, W. (1996) Hydrophobic interactions control zymogen activation in the trypsin family of serine proteases, *Biochemistry 35*, 4515−4523.
44. Bode, W. (1979) The transition of bovine trypsinogen to a trypsin-like state upon strong ligand binding, II. The binding of the pancreatic trypsin inhibitor and of isoleucine-valine and of sequentially related peptides to trypsinogen and to *p*-guanidinobenzoate-trypsinogen, *J. Mol. Biol. 127*, 357−374.
45. Stroud, R. M., Kossiakoff, A. A., and Chambers, J. L. (1977) Mechanisms of zymogen activation, *Annu. Rev. Biophys. Bioeng. 6*, 177−193.
46. McConn, J., Fasman, G. D., and Hess, G. P. (1969) Conformation of the high pH form of chymotrypsin, *J. Mol. Biol. 39*, 551−562.
47. Fersht, A. R., and Requena, Y. (1971) Equilibrium and rate constants for the interconversion of two conformations of α-chymotrypsin: the existence of a catalytically inactive conformation at neutral pH, *J. Mol. Biol. 60*, 279−290.
48. Fersht, A. R. (1972) Conformational equilibria in α- and δ-chymotrypsin: the energetics and importance of the salt bridge, *J. Mol. Biol. 64*, 497−509.
49. Hallgren, J., Spillmann, D., and Pejler, G. (2001) Structural requirements and mechanism for heparin-induced activation of a recombinant mouse mast cell tryptase, mouse mast cell protease-6, *J. Biol. Chem. 276*, 42774−42781.
50. De Young, M. B., Nemeth, E. F., and Scarpa, A. (1987) Measurement of internal pH of mast cell granules using microvolumetric fluorescence and isotopic techniques, *Arch. Biochem. Biophys. 254*, 222−233.
51. Whitaker-Menezes, D., Schechter, N. M., and Murphy, G. F. (1995) Serine proteinases are regionally segregated within mast cell granules, *Lab. Invest. 72*, 34−41.
52. Humphries, D. E., Wong, G. W., Friend, D. S., Gurish, M. F., Qui, W.-T., Huang, D., Sharpe, A. H., and Stevens, R. L. (1999) Heparin is essential for the storage of specific granule proteases in mast cells, *Nature 400*, 769−772.
53. Elrod, K. C., Moore, W., Abraham, W. M., and Tanaka, R. (1997) Lactoferrin, a potent tryptase inhibitor, abolishes late-phase airway response in allergic sheep, *Am. J. Respir. Crit. Care Med. 156*, 375−381.
54. Lindstedt, K. A., Kokkonen, J. O., and Kovanen, P. T. (1998) Regulation of the activity of secreted human lung mast cell tryptase by mast cell proteoglycans, *Biochim. Biophys. Acta 1452*, 617−627.

BI7004625